1

Endpoint and Epitope-specific Antibody Responses as Correlates of Vaccine-mediated Protection of Mice against Ricin Toxin

Greta Van Slyke[1,†], Dylan J Ehrbar[1, †], Jennifer Doering[1], Jennifer L. Yates[1], Ellen S.Vitetta[2], Oreola Donini[3], and Nicholas J Mantis[1,*]

[1]Division of Infectious Disease, Wadsworth Center, New York State Department of Health, Albany, NY 12208; [2]Department of Immunology and Microbiology, University of Texas Southwestern Medical School, Dallas, TX; [3]Soligenix, Inc., Princeton, NJ, 08540

*Corresponding Author: Division of Infectious Disease, Wadsworth Center, 120 New Scotland Avenue, Albany, NY 12208 Phone: 518-473-7487; Email: nicholas.mantis@health.ny.gov

[†], These authors contributed equally to this work.

1

ABSTRACT

25

26   The successful licensure of vaccines for biodefense is contingent upon the availability of

27 well-established correlates of protection (CoP) in at least two animal species that can then be

28 applied to humans, without the need to assess efficacy in the clinic. In this report we describe a

29 multivariate model that combines pre-challenge serum antibody endpoint titers (EPT) and values

30 derived from an epitope profiling immune-competition capture (EPICC) assay as a predictor in

31 mice of vaccine-mediated immunity against ricin toxin (RT), a Category B biothreat. EPICC is a

32 modified competition ELISA in which serum samples from vaccinated mice were assessed for

33 their ability to inhibit the capture of soluble, biotinylated (b)-RT by a panel of immobilized

34 monoclonal antibodies (mAbs) directed against four immunodominant toxin-neutralizing regions

35 on the enzymatic A chain (RTA) of RT. In a test cohort of mice (n=40) vaccinated with

36 suboptimal doses of the RTA subunit vaccine, RiVax®, we identified two mAbs, PB10 and

37 SyH7, which had EPICC inhibition values in pre-challenge serum samples that correlated with

38 survival following a challenge with 10 x LD_{50} of RT administered by intraperitoneal (IP)

39 injection. Analysis of a larger cohort of mice (n=645) revealed that a multivariate model

40 combining endpoint titers and an epitope-profiling immune-competition capture (EPICC) assay

41 values for PB10 and SyH7 as predictive variables had significantly higher statistical power than

42 any one of the independent variables alone. Establishing the correlates of vaccine-mediated

43 protection in mice represents an important steppingstone in the development of RiVax® as a

44 medical countermeasure under the United States Food and Drug Administration's "Two Animal

45 Rule."

46

47   **Keywords:** ricin; mouse; antibody; neutralizing; epitope; vaccine; biodefense

48

49   **Abbreviations:** Enzyme-linked immunosorbent assay (ELISA), epitope profiling immune-

50   competition capture (EPICC); Monoclonal antibody (mAb); biotinylated (b), ricin toxin (RT),

51   RT A chain (RTA)

52

1. Introduction

54   The development of vaccines to counteract biothreats, including toxins, remains a high
priority in many countries, including the United States [1, 2]. There are, however, formidable
challenges to development and licensure [3]. Foremost is the need to assess vaccine efficacy
(VE) in humans in the absence of clinical outcomes, because conventional efficacy studies are
not ethical and field trials are not feasible for most if not all the Category A and B Biothreats.
Under the Two Animal Rule, however, the United States Food and Drug Administration (FDA)
will evaluate VE based on "adequate and well-controlled studies in animal models of the human
disease or condition of interest" [4]. Of utmost importance are well-established and robust
correlates of protection (CoP) that apply across species and and can be applied to humans. The
undertaking of cross-species bridging studies has been successfully applied to anthrax vaccine
adsorbed (AVA) to estimate survival probabilities in vaccinated human populations [5].

65   RT is classified by the Centers for Disease Control and Prevention (CDC) as a Category
B biothreat, due to its extreme toxicity and ease by which it can be procured from castor beans
(*Ricinus communis*), which are cultivated globally for industrial and cosmetic applications. In its
mature form, RT is a ~65 kDa heterodimeric glycoprotein consisting of an RNA N-glycosidase
(RTA) joined by a disulfide to galactose/N-acetyl galactosamine (Gal/GalNAc)-specific lectin
(RTB). RTB facilitates ricin endocytosis and retrograde transport from the plasma membrane to
the endoplasmic reticulum (ER). Within the ER, RTA is released from RTB and retro-
translocated into the cytoplasm, where it functions as a ribosome-inactivating protein (RIP) by
depurinating a single residue in the sarcin-ricin loop (SRL) of 28S rRNA [6]. On the cellular
level, ribosome arrest triggers the ribotoxic-stress response (RSR) and activates stress-activated
protein kinase (SAPK) and programmed cell death (PCD) pathways [7]. The lethality of RT in
animals translates into a multifaceted pathophysiology initiated by cellular damage and driven by
inflammatory cytokines and death.

78   Historically, there are two advanced RTA-based subunit vaccines in development as a
medical countermeasures (MCM) for RT intoxication, RV*Ec* and RiVax® [8-10]. RV*Ec* is a
truncated version of RTA that lacks the molecule's C-terminal folding domain (residues 199-
267), as well as a small hydrophobic loop in the N-terminus (residues 34-43) [11-13]. RV*Ec* was
under development by the Department of Defense [8]. RiVax® and is a full-length variant (267

3

83   residues) of RTA with point mutations at position Y80 to disrupt RTA's RNA N-glycosidase

84   activity and V76 that eliminates RTA's ability to induce vascular leak syndrome (VLS) [14-16].

85   Pilot phase I clinical trials have indicated that both RV*Ec*- and RiVax®-adsorbed to aluminum

86   salt adjuvants are safe and immunogenic in healthy adults [8, 10]. Moreover, the efficacy of the

87   two vaccines has been demonstrated in animal models, including mice, and non-human primates

88   (NHPs) [16-19]. In the case of RiVax®, for example, Rhesus macaques vaccinated three times by

89   the intramuscular (IM) route at monthly intervals were immune to 3 x LD_{50} or aerosolized RT

90   [18]. In mice, RiVax® vaccination by intramuscular (IM), intraperitoneal (IP), subcutaneous (SC)

91   and intradermal (ID) protects against hyper-lethal doses of RT administered by inhalation,

92   gavage, or injection [19-22].

93   Despite the demonstrated pre-clinical efficacy of RiVax® and RV*Ec*, a CoP for RT has

94   not been formally established. Toxin-neutralizing antibody (TNA) titers are an obvious metric

95   and are used as the universal standard in assessing immunity to tetanus and diphtheria toxins [23,

96   24]. Unfortunately, in the case of RT, TNA assays are insensitive, difficult to standardize, and of

97   limited relevance to the primary cell types affected by RT *in vivo* (*e.g.*, alveolar macrophages,

98   Kupffer cells) [19]. However, it was reported that in a cohort of ~300 mice vaccinated with

99   RiVax® by the intradermal (ID) or intramuscular (IM) routes that animals that survived lethal

100   dose RT challenge had significantly higher RTA-specific serum IgG titers than those that died

101   [25]. Other reports have noted a similar association [19, 22] but none have rigorously evaluated

102   whether pre-challenge endpoint titers (EPT) are in fact predictive of survival.

103   In a recent study we raised the possibility that toxin-neutralizing, epitope-specific serum

104   IgG titers might serve as a relative correlate of protection [22]. In the case of RT there is

105   considerable evidence that toxin-neutralizing antibodies constitute only a fraction of the total

106   antibody pool elicited following RiVax® vaccination and that neutralizing antibodies target a

107   limited number of immunodominant epitopes on RTA, referred to as epitope clusters I-IV [26].

108   In the past several years, we have amassed a collection of mAbs and camelid-derived single

109   chain antibodies (V_HHs) against RTA that we have started to use as tools to investigate the

110   polyclonal response elicited by RiVax® antisera [18, 22, 26, 27]. Although we do not yet have a

111   full understanding of the relative importance of epitope-specific antibodies in contributing to

112   vaccine-induced immunity, passive protection studies in mice and NHP have indicated that

4

113   single mAbs or combinations of mAbs are sufficient to afford immunity to levels similar to those

114   achieved through active vaccination [28-31].

115   In this report, we explored EPT as well as values derived from an epitope profiling

116   immune-competition capture (EPICC) assay as possible correlates of vaccine-mediated

117   protection of mice against a lethal RT challenge dose by IP injection. The results demonstrate

118   that EPT and EPICC values each afforded significant power in predicting survival, but that a

119   multivariate model combining both metrics (i.e., EPT and EPICC values) improved

120   predictability. The EPICC assay has the benefit to being species neutral and therefore potentially

121   applicable across species as a possible co-correlate of immunity to RT.

122

123   **2. Material and Methods**

124   *2.1 Chemicals and biological reagents.*

125   RT; *Ricinus communis* agglutinin II; RCA_{60}) and biotin (b)-RT were purchased from

126   Vector Laboratories (Burlingame, CA). A thermostable batch of RiVax® was provided by

127   Soligenix, Inc (Princeton, NJ), as described [18]. The murine mAbs used in this study were

128   affinity purified from serum-free hybridoma supernatants using protein G chromatography at the

129   Dana Farber Cancer Institute Monoclonal Antibody Core facility (Boston, MA). Unless noted

130   otherwise, chemicals were obtained from the Sigma-Aldrich Company (St. Louis, MO).

131

132   *2.2 Mouse vaccination and RT challenge studies.*

133   Mouse experiments were conducted in strict accordance with protocol #18-384 approved

134   by the Wadsworth Center's Institutional Animal Care and Use Committee (IACUC). The

135   Wadsworth Center is an American Association for Laboratory Animal Science (AALAS)

136   accredited institution. Female BALB/c mice (IMSR Cat# TAC:balb, RRID:IMSR_TAC:balb; 8-

137   12-week old) were purchased from Taconic Biosciences (Rensselaer, NY) and housed at the

138   Wadsworth Center under conventional specific pathogen-free conditions. Mouse vaccinations

139   and RT challenges were carried out as reported previously [22]. Mice were immunized with

140   RiVax® (0.3, 1 or 3 µg) administered SC on days 0 (prime) and 21 (boost) [22]. Sera were

141   harvested by submandibular bleeding on day 30. Mice were challenged by IP injection with 5 x

142   LD_{50} RT (~1 µg/mouse; 10 µg/kg) on study day 35 and monitored for 7 days thereafter for

143   morbidity and weight loss.

144

145   *2.3 ELISA.*

146   Indirect and competitive capture ELISAs were performed as described [22]. Nunc

147   Maxisorb F96 microtiter plates (Thermo Scientific, Pittsburgh, PA) were coated with RT (1

148   µg/ml in PBS, pH 7.4) overnight at 4°C. The plates were blocked with phosphate buffered saline

149   (PBS) containing goat serum (2% v/v; Gibco, Grand Island, NY) and Tween-20 (0.1% v/v).

150   Serum samples were serially (1:2) diluted in blocking solution. Horseradish peroxidase (HRP)-

151   labeled goat anti-mouse IgG polyclonal antibodies (SouthernBiotech, Birmingham, AL) were

152   used as secondary antibodies. TMB (3,3′,5,5′-tetramethylbenzidine; Kirkegaard & Perry Labs,

153   Gaithersburg, MD) was used as colorimetric detection substrate and reactions were stopped with

154   1 N phosphoric acid. Plates were read on a SpectroMax 250 spectrophotometer and analyzed

155   with Softmax Pro 5.4.5 software (Molecular Devices, Sunnyvale, CA). End-point titers were

156   defined as the dilution where absorbance >3-times above the background *(e.g.,* blank wells).

157   Seroconversion was defined as an endpoint titer in a RT ELISA of $\geq$ 1:50. Geometric mean

158   titers (GMTs) were calculated from the endpoint titers. Mice that had not seroconverted, as

159   determined by ELISA, were assigned a GMT of 1 for the purposes of statistical analysis.

160

161   *2.3 Epitope profiling immune-competition capture (EPICC) assay.*

162   Immulon 4HBX 96-well microtiter plates (Thermo Scientific) were coated with indicated

163   anti-RTA mAbs (1 µg/ml in 0.1 mL) in PBS, pH 7.4 at room temperature for 1 h and then

164   blocked overnight at 4°C, as noted above. For EPICC, the amount of b-RT used in the assay was

165   adjusted to the EC$_{90}$ for each MAbs (30-200 ng/ml) [32], as shown in **Table 1**. Serial dilutions of

166   control or immune sera were mixed with b-RT (EC$_{90}$) in duplicate in PVC microtiter plates,

167   incubated for 15 min and then transferred using a multichannel pipette to Immulon 4HBX 96-

168   well microtiter plates (Thermo Scientific) coated with indicated anti-RTA mAbs (1 µg/ml in 0.1

169   mL). in PBS, pH 7.4 at room temperature for 1 h and then blocked overnight at 4°C, as noted

170   above. As controls, each mAb (10 µg/ml) was competed with itself to establish a 100%

171   inhibitory baseline. The microtiter plates were incubated at RT for 1 h, washed and then probed

172   with streptavidin-HRP (1ug/ml; Thermo Scientific) and developed with 3,3′,5,5′-

173   Tetramethylbenzidine (TMB) (Kirkegaard & Perry Labs). Plates were analyzed with a

174   SpectroMax 250 spectrophotometer using Softmax Pro 5.2 software (Molecular Devices).

6

175   Inhibition of RT binding was calculated as a percentage of b-RT binding to the coated MAb,

176   where: $[100-(OD_{450}C/OD_{450}B)*100]$= % RT binding inhibited by competitor, and C= competed

177   well, B= b-R (EC_{90}). Pooled sera from RiVax-vaccinated rabbits and Rhesus macaques [18]

178   were diluted in PBS prior to use for EPICC analysis.

179

180   *2.3 Statistical analysis.*

181   Endpoint titers were log-transformed prior to statistical analysis. Endpoint titers were

182   compared using one-way analysis of variance (ANOVA) followed by Dunnett's multiple

183   comparison test. Survival data were tested using the log rank Mantel-Cox test. In all cases the

184   significance threshold was set at $P < 0.05$. ANOVA and log rank tests were performed using

185   GraphPad Prism v. 8.0 for Windows (GraphPad Software, San Diego, CA, USA).

186   Correlations between endpoint titers or EPICC values and mouse survival following

187   challenge with RT were determined by simple logistic regression. In the initial cohort of 40

188   mice, the optimal set of predictive variables was defined using least absolute shrinkage and

189   selection operator (LASSO) penalized logistic regression [33]. Ten-fold cross-validation was

190   performed 10 times to select the optimal values for the λ penalty parameter. All sets of values for

191   each separate potential correlate of protection were standardized to a mean of 0 and a standard

192   deviation of 1 before LASSO regression. The selected variables were then measured in the mice

193   included in subsequent experiments and included in analysis of the larger dataset of 645 mice.

194   The predictive performance of each model constructed from the larger dataset was

195   assessed by receiver operating characteristic (ROC) analysis, which allowed us to examine the

196   trade-off between sensitivity and specificity along the entire range of values for each variable.

197   The area under the curve (AUC) was also used as a measure of the predictive value of each

198   variable, while Delong's test was used to compare the AUC of each model [34]. P-values

199   resulting from Delong's test were adjusted for multiple comparisons with the Holm-Sidak

200   method. Analyses were performed in R 3.4.2 [35], the R package pROC for ROC analysis [36],

201   and the R package glmnet for LASSO penalized logistic regression [37].

202

203   **3. Results**

204   *3.1 Probing RiVax® with mAbs directed against four spatially distinct toxin-neutralizing epitope*

205   *clusters.*

206   We previously described four spatially distinct immunodominant B cell epitope clusters

207   (I-IV) on RiVax® [26, 27, 38]. Each cluster is defined by one or more RT-neutralizing mAbs

208   (**Table 1**). Cluster I, defined by PB10, is focused around RTA's α-helix B (residues 94-107), a

209   protruding element previously known to be a target of potent RT-neutralizing antibodies [39,

210   40]. Cluster II, defined by SyH7 and PA1, is located on the back side of RTA, relative to the

211   active site pocket [26]. Cluster III is targeted by MAb IB2 and is in close proximity to RTA's

212   active site [41]. Finally, Cluster IV, defined by GD12, forms a diagonal sash from the front to

213   back of the subunit. We previously reported that antisera from NHPs and humans vaccinated

214   with RiVax® competes with mAbs from cluster I (PB10) and cluster II (SyH7, PA1) for binding

215   to RT [18].

216   We performed cross-competition capture ELISAs with each of the eight representative

217   mAbs as confirmation that the four epitope clusters are spatially distinct (**Table 1**). In this

218   modified capture ELISA, microtiter plates were coated with individual mAbs and probed with

219   soluble b- RT, in the absence or presence of a competitor mAb. A reduction in the capture of

220   soluble b-RT in the presence of a competitor was interpreted as epitope overlap or steric

221   hindrance [42]. We refer to this modified competition ELISA as EPICC.

222   As shown in **Figure 1**, there was across the board intra-cluster competition, with only

223   limited inter-cluster competition. For example, cluster II mAbs, SyH7, PA1, PH12 and TB12,

224   competed with each other, but not with mAbs in clusters I, III, or IV. Similarly, IB2 (cluster III)

225   competed with itself but not with the other seven mAbs. The exception was competition between

226   GD12 (cluster IV), and two cluster I mAbs, PB10 and R70. This cross-cluster competition (I

227   versus III) is attributed to the contact of GD12 with the α-helix B [26]. JD4, the other cluster IV

228   mAb in our collection, did not compete with PB10 or R70. These results demonstrate our ability

229   to "interrogate" specific immunodominant epitope clusters on RiVax® by competition ELISA.

230   To examine whether the epitope-specific antibodies against the 4 clusters identified in

231   mice are also present in other species, we performed EPICC analysis with pooled immune sera

232   from rabbits and Rhesus macaques that had been vaccinated with RiVax™. As shown in **Figure**

233   **2**, pooled sera from all three species competed with the murine mAbs representing clusters I

234   (PB10, WECB2), II (PA1, SyH7, PH12, TB12), III (IB2), and IV (GD12). These results

235   demonstrate that the four immunodominant epitope clusters on RTA identified in mice are also

236   targets of antibodies in other species.

8

237

238 *3.2 Preliminary analysis of EPT and EPICC values as correlates of vaccine-mediated protection.*

239   We next investigated the relative importance of RT-specific serum IgG titers and EPICC

240 values as predictors of survival following a lethal injection of RT. To generate a preliminary

241 data set, a group of 40 mice were divided into two cohorts and vaccinated SC on days 0 and 21

242 with RiVax® at optimal (1 µg; cohort 1) or sub-optimal (0.3 µg; cohort 2) doses. Serum samples

243 were collected on day 30, and the mice were challenged on day 35 with 5 x LD_{50} of RT

244 administered by IP injection. Mice were then monitored for 7 days post-challenge for weight loss

245 and morbidity, as described [38]. The results of each mouse in that experiment are presented in

246 **Appendix 1**.

247   In cohort 1, 19 of the 20 vaccinated mice (95%) survived RT challenge, whereas in

248 cohort 2 only 9 out of 20 survived (45%). As shown in **Figure 3**, pre-challenge, RT-specific EPT

249 were significantly higher in mice that survived RT exposure (n=12), as compared to the

250 decedents (median = 4.408 log_{10} transformed EPT for the survivors vs. 3.204 for the decedents,

251 U = 72.50, P = 0.0033, as determined by two-tailed Mann-Whitney U test). In terms of pre-

252 challenge EPICC analysis, mice that survived RT challenge had significantly higher PB10

253 (median = 29.4% inhibition for survivors vs. 9.8% for decedents, U = 65, P = 0.0017), SyH7

254 (median = 10.2% for survivors vs. 4.95% for decedents, U = 97, P = 0.0362), and PH12 (median

255 = 16.43% for survivors vs. 4.782 for decedents, U = 94, P = 0.0286) inhibition values as

256 compared to the decedents. In contrast, EPICC values for IB2 (P = 0.1631) and GD12 (P =

257 0.6308) were not significantly different between groups of mice that survived or died (**Figure 3**).

258   We next generated a series of univariate logistic regression models to further examine the

259 relationships between survival and pre-challenge, RT-specific serum EPT and EPICC. Logistic

260 regression demonstrated a significant relationship between EPT and survival (pP < 0.01). For the

261 EPICC analysis, inhibitory levels of each of the five RTA-specific mAbs was designated as the

262 independent variable and death was designated as the dependent variable. For PB10 and SyH7,

263 there was a significant correlation between EPICC values and survival, whereas for PH12, IB2,

264 and GD12 there was not. To assess the predictive performance of the logistic regression models

265 we employed ROC analysis. The models yielded AUC values of 0.7842 for EPT, 0.8065 for

266 PB10 inhibition and 0.7113 for SyH7 inhibition. LASSO penalized logistic regression selected

267 the optimal set of predictive variables as being EPT, combined with PB10 and SyH7 EPICC

9

268   inhibition values. Thus, combining EPT and EPICC values derived from PB10 or SyH7 was

269   tentatively the most effective predictor of immunity to a lethal dose of injected RT.

270

271   *3.3 A multivariant model combining EPT and EPICC as a correlate of vaccine-mediated*

272   *protection.*

273   We next examined a much larger cohort of mice (n=645) that had been uniformly

274   vaccinated with RiVax® on days 0 and 21, and then challenged with a 5x LD_{50} dose of RT on

275   day 35 [22]. Serum samples were collected from the animals five days prior (day 30) to the

276   challenge. Within this cohort, 374 mice survived ricin challenge and 271 died (**Appendix 2**).

277   In accordance with the preliminary study, RT-specific IgG titers in sera collected on day

278   30 were higher in the mice that subsequently survived a lethal dose, as compared to mice that

279   succumbed (median = 3.607 $\log_{10}$ transformed EPT for survivors vs. 1.699 for decedents, $U =$

280   12245, P < 0.0001, as determined by two-tailed Mann-Whitney U test; **Figure 5A**). Similarly,

281   EPICC revealed that mice that survived the challenge had significantly higher PB10 (median =

282   41.95% inhibition for survivors vs. 3.244 for decedents, $U =$ 17659, P < 0.0001) and SyH7

283   inhibition values (median = 19.70% for survivors vs. 1.001% for decedents, $U =$ 19069, P <

284   0.0001), as compared to the decedents (**Figure 5 B,C**). Moreover, all 3 variables correlated with

285   survival when examined in the single-variable models (P < 2e-16 for all) (**Table 3**; **Figure 6**).

286   The univariate EPT model had the highest AUC of the three (0.8792, 95% CI 0.8526-0.9057),

287   followed by PB10 (0.8258, 95% CI 0.7939-0.8576) and SyH7 (0.8119, 95% CI 0.779-0.8447).

288   The AUC values for PB10 and SylH3 were each were significantly lower than the AUC derived

289   from EPT (Holm-Šídák adjusted P < 0.05, as determined by Delong's test), demonstrating that

290   when considering univariate analysis EPT is superior. However, a multivariate model

291   considering EPT and EPICC for PB10 and SyH7 as predictive variables had a significantly

292   higher AUC (0.901, 95% CI 0.8773-0.9246) than did EPT alone (Holm-Šídák adjusted P < 0.05)

293   (**Table 3**). In summary, EPT and EPICC values for both PB10 and SyH7 have the potential to

294   serve as co-correlates of vaccine-mediated protection of mice against RT with the term "co-

295   correlate" being defined by Plotkin as "…a quantity of a specific immune response to a vaccine

296   that is 1 of >2 correlates of protection and that may be synergistic with other correlates." [23]

297

298   **4. Discussion**

299   In this report we investigated in a mouse model the potential of pre-challenge, RT-

300   specific serum EPTs, as well as RTA epitope-specific antibody levels, to serve as CoP from

301   lethal dose ricin toxin challenge, administered by injection. In both a pilot and larger cohort of

302   mice, EPT emerged as having significant predictive value as a CoP. This finding unto itself

303   constitutes an advance in the development of RiVax® considering that EPTs have never been

304   formally been evaluated for its prognostic use with survival as an endpoint. By the same token,

305   EPICC values derived using two mAbs, PB10 and SyH7, directed against different

306   immunodominant toxin-neutralizing epitopes on RTA, were also significantly predictive of

307   survival in the mouse model. Combining EPT and RTA-specific epitope reactivity, as

308   determined by EPICC, ultimately provided the highest predictive power.

309   It should be noted that one advantage of the EPICC assay over direct competition

310   ELISAs is that it is species neutral, because it relies on the detection of captured biotinylated

311   ricin toxin using avidin-HRP, rather than using species-specific secondary reagents. This enables

312   direct cross-species comparisons in pre-clinical testing. Another advantage is that EPICC

313   involves the capture soluble antigen (RT), rather than detection of antigen immobilized on

314   polystyrene microtiter wells. This is biologically significant because RT and its individual toxin

315   subunits are partially denatured on plastic surfaces, resulting in the exposure of cryptic epitopes

316   and possibly perturbation of native secondary structures.

317   We have recently initiated studies in Rhesus macaques to evaluate the bridging of

318   potential of EPT and EPICCs as indicators of RiVax® -induced protection against RT. As alluded

319   to above, it was previously demonstrated that Rhesus macaques that received three IM

320   vaccinations with RiVax® (100 μg/dose) on days 0, 30, and 60 were protected against a 3 x LD_{50}

321   toxin challenge by aerosol on day 110 [18]. In that study, serum samples were assessed for RT-

322   specific EPT, TNA, and preliminary competition ELISAs with a subset of RTA-specific mAbs,

323   including PB10 and SyH7. However, establishing a CoP from that experiment alone was not

324   possible considering that all animals survived ricin challenge (except for one that died from

325   causes unrelated to toxin exposure). Nonetheless, that report and the work presented in Figure 2

326   of this study bodes well for the applicability of EPICC to the NHP model, in that the four RT-

327   neutralizing immunodominant epitopes on RTA identified in mice appear to be shared across

328   species. Whether the specific EPICC profiles will translate across species is under evaluation. In

329   our current study, PB10 and SyH7 inhibition values, representing epitope clusters I and II,

330   elicited following RiVax vaccination were predictive of survival. However, in preliminary

331   analysis of NHP samples, IB2, representing cluster III, and not PB10 or SyH7 appear to correlate

332   with protection (G. Van Slyke, D Ehrbar, C. Roy E. Vitetta, N. Mantis, unpublished results).

333   It should be noted that the conclusions drawn from our current study are limited to a

334   single vaccination route (SC) and a single challenge route (IP). It is possible that specific CoPs

335   for RT may depend on the site of vaccination and the mode of toxin exposure. Inhalation of RT

336   triggers a particularly complex pathophysiology that results in acute lung injury (ALI) and acute

337   respiratory distress syndrome (ARDS) involving multiple different cell types and inflammatory

338   cytokines [43-45]. It is unclear where and how antibodies function to protect the lung against

339   RT-induced damage, although a recent report from our group demonstrated that a humanized

340   version of PB10 is sufficient, when given prophylactically by intravenous infusion, to protect

341   Rhesus macaques against aerosolized ricin [31]. Thus, there are at least some parallels between

342   rodents and NHPs, considering that PB10 has comparable toxin-neutralizing efficacy in mice as

343   NHPs [46].

344   In summary, we have described a multivariate model combining EPT and EPICC values

345   that affords high confidence in predicting survival of mice following a lethal challenge with RT.

346   This model should facilitate the development of RiVax® as a MC for RT under the United States

347   Food and Drug Administration's "Animal Rule."

348

356

357   **Author Contributions (CRediT): GVS, NJM**: conceptualization; **GVS, DJE, JW, and JY**:

358   investigation; **GVS, DJE, DJV, EV, OD, NJM**: formal analysis; **GVS, DJE NJM**: writing

359   original draft: **EV, OD, NJM**: writing, review and editing; **NJM:** Supervision and project

360   administration.

361

Declaration of Interest statement: GVS, DJE, JW, JY, EV, and NJM declare no competing

interests. OD is an employee of Soligenix, Inc. which holds the license for RiVax®.

364

References Cited

[1] De Groot AS, Moise L, Olive D, Einck L, Martin W. Agility in adversity: Vaccines on
Demand. Expert Rev Vaccines. 2016;15:1087-91.

[2] Larsen JC, Disbrow GL. Project BioShield and the Biomedical Advanced Research
Development Authority: A ten year progress report on meeting U.S. preparedness objectives
for threat agents. Clin Infect Dis. 2017.

[3] Williamson ED, Duchars MG, Kohberger R. Predictive models and correlates of protection
for testing biodefence vaccines. Expert Rev Vaccines. 2010;9:527-37.

[4] Approval of Biological Products When Human Efficacy Studies Are Not Ethical or Feasible

[5] Stark GV, Sivko GS, VanRaden M, Schiffer J, Taylor KL, Hewitt JA, et al. Cross-species
prediction of human survival probabilities for accelerated anthrax vaccine absorbed (AVA)
regimens and the potential for vaccine and antibiotic dose sparing. Vaccine. 2016;34:6512-7.

[6] Endo Y, Tsurugi K. RNA N-glycosidase activity of ricin A-chain. Mechanism of action of
the toxic lectin ricin on eukaryotic ribosomes. J Biol Chem. 1987;262:8128-30.

[7] Lee MS, Tesh VL. Roles of Shiga Toxins in Immunopathology. Toxins (Basel). 2019;11.

[8] Pittman PR, Reisler RB, Lindsey CY, Guerena F, Rivard R, Clizbe DP, et al. Safety and
immunogenicity of ricin vaccine, RVEc, in a Phase 1 clinical trial. Vaccine. 2015;33:7299-
306.

[9] Vance DJ, Mantis NJ. Progress and challenges associated with the development of ricin toxin
subunit vaccines. Expert Rev Vaccines. 2016;15:1213-22.

[10] Vitetta ES, Smallshaw JE, Schindler J. Pilot phase IB clinical trial of an alhydrogel-
adsorbed recombinant ricin vaccine. Clin Vaccine Immunol. 2012;19:1697-9.

[11] Carra JH, Wannemacher RW, Tammariello RF, Lindsey CY, Dinterman RE, Schokman
RD, et al. Improved formulation of a recombinant ricin A-chain vaccine increases its stability
and effective antigenicity. Vaccine. 2007;25:4149-58.

[12] McHugh CA, Tammariello RF, Millard CB, Carra JH. Improved stability of a protein
vaccine through elimination of a partially unfolded state. Protein Sci. 2004;13:2736-43.

392   [13] Olson MA, Carra JH, Roxas-Duncan V, Wannemacher RW, Smith LA, Millard CB. Finding

393   a new vaccine in the ricin protein fold. Protein Eng Des Sel. 2004;17:391-7.

394   [14] Smallshaw JE, Firan A, Fulmer JR, Ruback SL, Ghetie V, Vitetta ES. A novel recombinant

395   vaccine which protects mice against ricin intoxication. Vaccine. 2002;20:3422-7.

396   [15] Smallshaw JE, Ghetie V, Rizo J, Fulmer JR, Trahan LL, Ghetie MA, et al. Genetic

397   engineering of an immunotoxin to eliminate pulmonary vascular leak in mice. Nat Biotechnol.

398   2003;21:387-91.

399   [16] Smallshaw JE, Richardson JA, Pincus S, Schindler J, Vitetta ES. Preclinical toxity and

400   efficacy testing of RiVax, a recombinant protein vaccine against ricin. Vaccine.

401   2005;23:4775-84.

402   [17] McLain DE, Lewis BS, Chapman JL, Wannemacher RW, Lindsey CY, Smith LA.

403   Protective effect of two recombinant ricin subunit vaccines in the New Zealand white rabbit

404   subjected to a lethal aerosolized ricin challenge: survival, immunological response, and

405   histopathological findings. Toxicol Sci. 2012;126:72-83.

406   [18] Roy CJ, Brey RN, Mantis NJ, Mapes K, Pop IV, Pop LM, et al. Thermostable ricin vaccine

407   protects rhesus macaques against aerosolized ricin: Epitope-specific neutralizing antibodies

408   correlate with protection. Proc Natl Acad Sci U S A. 2015;112:3782-7.

409   [19] O'Hara JM, Brey RN, 3rd, Mantis NJ. Comparative efficacy of two leading candidate ricin

410   toxin a subunit vaccines in mice. Clin Vaccine Immunol. 2013;20:789-94.

411   [20] Smallshaw JE, Richardson JA, Vitetta ES. RiVax, a recombinant ricin subunit vaccine,

412   protects mice against ricin delivered by gavage or aerosol. Vaccine. 2007;25:7459-69.

413   [21] Smallshaw JE, Vitetta ES. A lyophilized formulation of RiVax, a recombinant ricin subunit

414   vaccine, retains immunogenicity. Vaccine. 2010;28:2428-35.

415   [22] Westfall J, Yates JL, Van Slyke G, Ehrbar D, Measey T, Straube R, et al. Thermal stability

416   and epitope integrity of a lyophilized ricin toxin subunit vaccine. Vaccine. 2018;36:5967-76.

417   [23] Plotkin SA. Vaccines: correlates of vaccine-induced immunity. Clin Infect Dis.

418   2008;47:401-9.

419   [24] Plotkin SA. Updates on immunologic correlates of vaccine-induced protection. Vaccine.

420   2020;38:2250-7.

421   [25] Marconescu PS, Smallshaw JE, Pop LM, Ruback SL, Vitetta ES. Intradermal administration
422   of RiVax protects mice from mucosal and systemic ricin intoxication. Vaccine. 2010;28:5315-
423   22.

424   [26] Toth RTI, Angalakurthi SK, Van Slyke G, Vance DJ, Hickey JM, Joshi SB, et al. High-
425   Definition Mapping of Four Spatially Distinct Neutralizing Epitope Clusters on RiVax, a
426   Candidate Ricin Toxin Subunit Vaccine. Clin Vaccine Immunol. 2017;24.

427   [27] Vance DJ, Tremblay JM, Rong Y, Angalakurthi SK, Volkin DB, Middaugh CR, et al. High-
428   Resolution Epitope Positioning of a Large Collection of Neutralizing and Nonneutralizing
429   Single-Domain Antibodies on the Enzymatic and Binding Subunits of Ricin Toxin. Clin
430   Vaccine Immunol. 2017;24.

431   [28] Noy-Porat T, Rosenfeld R, Ariel N, Epstein E, Alcalay R, Zvi A, et al. Isolation of Anti-
432   Ricin Protective Antibodies Exhibiting High Affinity from Immunized Non-Human Primates.
433   Toxins (Basel). 2016;8.

434   [29] Rong Y, Pauly M, Guthals A, Pham H, Ehrbar D, Zeitlin L, et al. A Humanized Monoclonal
435   Antibody Cocktail to Prevent Pulmonary Ricin Intoxication. Toxins (Basel). 2020;12.

436   [30] Rong Y, Torres-Velez FJ, Ehrbar D, Doering J, Song R, Mantis NJ. An intranasally
437   administered monoclonal antibody cocktail abrogates ricin toxin-induced pulmonary tissue
438   damage and inflammation. Hum Vaccin Immunother. 2019:1-15.

439   [31] Roy CJ, Van Slyke G, Ehrbar D, Bornholdt ZA, Brennan MB, Campbell L, et al. Passive
440   immunization with an extended half-life monoclonal antibody protects Rhesus macaques
441   against aerosolized ricin toxin. NPJ Vaccines. 2020;5:13-.

442   [32] Sebaugh JL. Guidelines for accurate EC50/IC50 estimation. Pharm Stat. 2011;10:128-34.

443   [33] Chen L, Schiffer JM, Dalton S, Sabourin CL, Niemuth NA, Plikaytis BD, et al.
444   Comprehensive analysis and selection of anthrax vaccine adsorbed immune correlates of
445   protection in rhesus macaques. Clin Vaccine Immunol. 2014;21:1512-20.

446   [34] DeLong ER, DeLong DM, Clarke-Pearson DL. Comparing the areas under two or more
447   correlated receiver operating characteristic curves: a nonparametric approach. Biometrics.
448   1988;44:837-45.

449   [35] R_Core_Team. R: A language and environment for statistical computing. Vienna, Austria:
450   R Foundation for Statistical Computing; 2014.

451   [36] Robin X, Turck N, Hainard A, Tiberti N, Lisacek F, Sanchez JC, et al. pROC: an open-
452   source package for R and S+ to analyze and compare ROC curves. BMC Bioinformatics.
453   2011;12:77.

454   [37] Friedman J, Hastie T, Tibshirani R. Regularization Paths for Generalized Linear Models via
455   Coordinate Descent. J Stat Softw. 2010;33:1-22.

456   [38] Van Slyke G, Angalakurthi SK, Toth RTt, Vance DJ, Rong Y, Ehrbar D, et al. Fine-
457   Specificity Epitope Analysis Identifies Contact Points on Ricin Toxin Recognized by
458   Protective Monoclonal Antibodies. Immunohorizons. 2018;2:262-73.

459   [39] Lemley PV, Amanatides P, Wright DC. Identification and characterization of a monoclonal
460   antibody that neutralizes ricin toxicity in vitro and in vivo. Hybridoma. 1994;13:417-21.

461   [40] O'Hara JM, Neal LM, McCarthy EA, Kasten-Jolly JA, Brey RN, 3rd, Mantis NJ. Folding
462   domains within the ricin toxin A subunit as targets of protective antibodies. Vaccine.
463   2010;28:7035-46.

464   [41] Angalakurthi SK, Vance DJ, Rong Y, Nguyen CMT, Rudolph MJ, Volkin D, et al. A
465   Collection of Single-Domain Antibodies that Crowd Ricin Toxin's Active Site. Antibodies
466   (Basel). 2018;7.

467   [42] Derking R, Ozorowski G, Sliepen K, Yasmeen A, Cupo A, Torres JL, et al. Comprehensive
468   antigenic map of a cleaved soluble HIV-1 envelope trimer. PLoS Pathog. 2015;11:e1004767.

469   [43] Pincus SH, Bhaskaran M, Brey RN, 3rd, Didier PJ, Doyle-Meyers LA, Roy CJ. Clinical and
470   Pathological Findings Associated with Aerosol Exposure of Macaques to Ricin Toxin. Toxins
471   (Basel). 2015;7:2121-33.

472   [44] Sapoznikov A, Falach R, Mazor O, Alcalay R, Gal Y, Seliger N, et al. Diverse profiles of
473   ricin-cell interactions in the lung following intranasal exposure to ricin. Toxins (Basel).
474   2015;7:4817-31.

475   [45] Sapoznikov A, Gal Y, Falach R, Sagi I, Ehrlich S, Lerer E, et al. Early disruption of the
476   alveolar-capillary barrier in a ricin-induced ARDS mouse model: neutrophil-dependent and -
477   independent impairment of junction proteins. Am J Physiol Lung Cell Mol Physiol.
478   2019;316:L255-L68.

479   [46] Van Slyke G, Sully EK, Bohorova N, Bohorov O, Kim D, Pauly MH, et al. Humanized
480   Monoclonal Antibody That Passively Protects Mice against Systemic and Intranasal Ricin
481   Toxin Challenge. Clin Vaccine Immunol. 2016;23:795-9.

482

Figure Legends

484

Figure 1. Spatial segregation of immunodominant neutralizing B cell epitopes on RTA, as determined by EPICC. Cross competition ELISAs with indicated mAbs used as capture (y-axis) or competitor (x-axis) in solution with b-RT. The heatmap scheme indicates percent inhibition of competitor MAb, as compared to b-RT alone with inset numbers indicating percent reduction in a representative experiment. Negative values indicate enhancement of b-RT-in capture.

491

Figure 2. EPICC analysis of antisera from rabbits and NHPs vaccinated with RiVax. Pooled polyclonal sera from RiVax® -vaccinated (A) mice, (B) rabbits and (C) Rhesus macaques were subjected to EPICC with mAbs (see inset legends in first column) directed against RTA epitope clusters I, II, III and IV.

496

Figure 3. Pilot study reveals EPT and EPICC as putative correlates of protection in a cohort of RiVax® vaccinated mice. Female BALB/c mice (n=40) were vaccinated with suboptimal or near optimal doses of RiVax® (0.3 or 1 μg) at days 0 and 21 and challenged with 10 x LD_{50} RT on day 35. Sera was collected from mice on day 30 and analyzed by (A) indirect ELISA to determine EPT and (B-F) EPICC analysis. Statistical significance between survivors and decedents is denoted by an asterisk (unpaired t test; $p < 0.02$).

503

Figure 4. EPT and EPICC values for SyH7 and PB10 as correlates of immunity to RT. Results presented in Figure 3 were subjected to variable selection using LASSO penalized logistic regression. LASSO coefficient profiles were generated for all potential correlates of protection: EPT, PB10, SyH7, PH12, IB2 and GD12. Each curve corresponds to a potential predictive variable with coefficients plotted against the L1 Norm regularization term (lower x-axis). The upper x-axis depicts the number of nonzero coefficients at the respective regularization parameter.

511

512 **Figure 5. EPT and EPICC as putative correlates of protection in a large cohort of RiVax®**

513 **vaccinated mice.** A cohort of 646 mice total vaccinated with RiVax® (dose range 0.3-3ug) on

514 days 0 and 21 were challenged with RT on day 35, as reported in **Appendix 2**. Violin plots of

515 pre-challenge serum samples examined for (A) EPT and (B-C) EPICC values with PB10 and

516 SyH7. Statistical significance between survivors and decedents is denoted by an asterisk (Mann-

517 Whitney test; p>0.0001).

518

519 **Figure 6. ROC curve analysis of predictive performance of classifying variables in the large**

520 **cohort.** Curves are based on univariate logistic regression models including the labeled variable.

521 Area under the curve (AUC) values and corresponding 95% confidence intervals are included for

522 each predictive variable.

523

524 **Tables**

525

Table 1. Mouse mAbs used for EPICC analysis			
Cluster	**MAb**	**K_D (x 10^{-12} M)**[a]	**EC_{90} (μg/ml)** [b]
I	PB10	1.24	0.1
	WECB2	3.10	0.03
II	SyH7	20.3	0.07
	PA1	9.19	0.03
	PH12	9.10	0.07
	TB12	44.2	0.05
III	IB2	49.3	0.25
IV	GD12	55.2	0.25

[a], apparent affinity of dissociation values from [26]; [b], Derived from b-RT competition values;

526

527

528

Table 2. Logistic regression analysis of EPICC and endpoint titers

Variable	IEC[a] (P value)	VEC[b] (P value)	AUC[c] (95% CI)	LASSO[d]
PB10	0.74005 (0.2381)	-0.08322 (0.0102)	0.8065 (0.6729-0.9402)	●
SyH7	0.16697 (0.7656)	-0.12298 (0.0373)	0.7113 (0.5297-0.8929)	●
PH12	-0.19418 (0.6786)	-0.04827 (0.0812)	0.7202 (0.5441-0.8963)	
GD12	-0.79588 (0.0289)	-0.01487 (0.6851)	0.5506 (0.3648-0.736)	
IB2	-0.35306 (0.3915)	-0.02873 (0.0601)	0.6429 (0.4482-0.8375)	
EPT	3.8963 (0.0405)	-1.2807 (0.0129)	0.7842 (0.6435-0.9249)	●

[a]IEC, Intercept estimated coefficient, [b]VEC, Variable estimated coefficient, [c]AUC, Area under the curve, [d]Variable selection by LASSO penalized logistic regression

529

Table 3. Model comparison as immune correlates of protection against RT in mice

Model	Variable	IEC[a] (P value)	VEC[b] (P value)	AUC[c] (95% CI)	P value for AUC vs EP titer[d]
SyH7		0.689023 (5.34e-09)	-0.091457 (< 2e-16)	0.8119 (0.779-0.8447)	**0.0004031**
PB10		0.82242 (1.85e-11)	-0.05578 (< 2e-16)	0.8258 (0.7939-0.8576)	**0.0041451**
$\log_{10}$ EP titer		2.78001 (<2e-16)	-1.17223 (<2e-16)	0.8792 (0.8526-0.9057)	N/A
SyH7 + PB10	SyH7	1.118649 (2.76e-16)	-0.058101 (3.15e-11)	0.8561 (0.8273-0.8849)	0.1047056
	PB10		-0.039627 (4.97e-15)		
SyH7 + EP	SyH7	2.684511 (< 2e-16)	-0.052147 (3.54e-09)	0.8938 (0.8692-0.9184)	0.0971708
	EP		-0.920670 (< 2e-16)		
PB10 + EP	PB10	2.600741 (< 2e-16)	-0.032372 (4.55e-10)	0.8933 (0.8682-0.9184)	0.1047056
	EP		-0.871628 (< 2e-16)		
SyH7 + PB10 + EP	SyH7	2.589035 (< 2e-16)	-0.036901 (9.33e-05)	0.901 (0.8773-0.9246)	**0.0135862**
	PB10		-0.023665 (2.03e-05)		
	EP		-0.778338 (4.58e-16)		

[a]IEC: Intercept estimated coefficient, [b]VEC: Variable estimated coefficient, [c]AUC: Area under the curve, [d]Delong's test p value (Holm-Šídák adjusted) comparing AUC to that of $\log_{10}$ transformed EP titer. Significant P values are bolded.

530

531

532

Figure 1
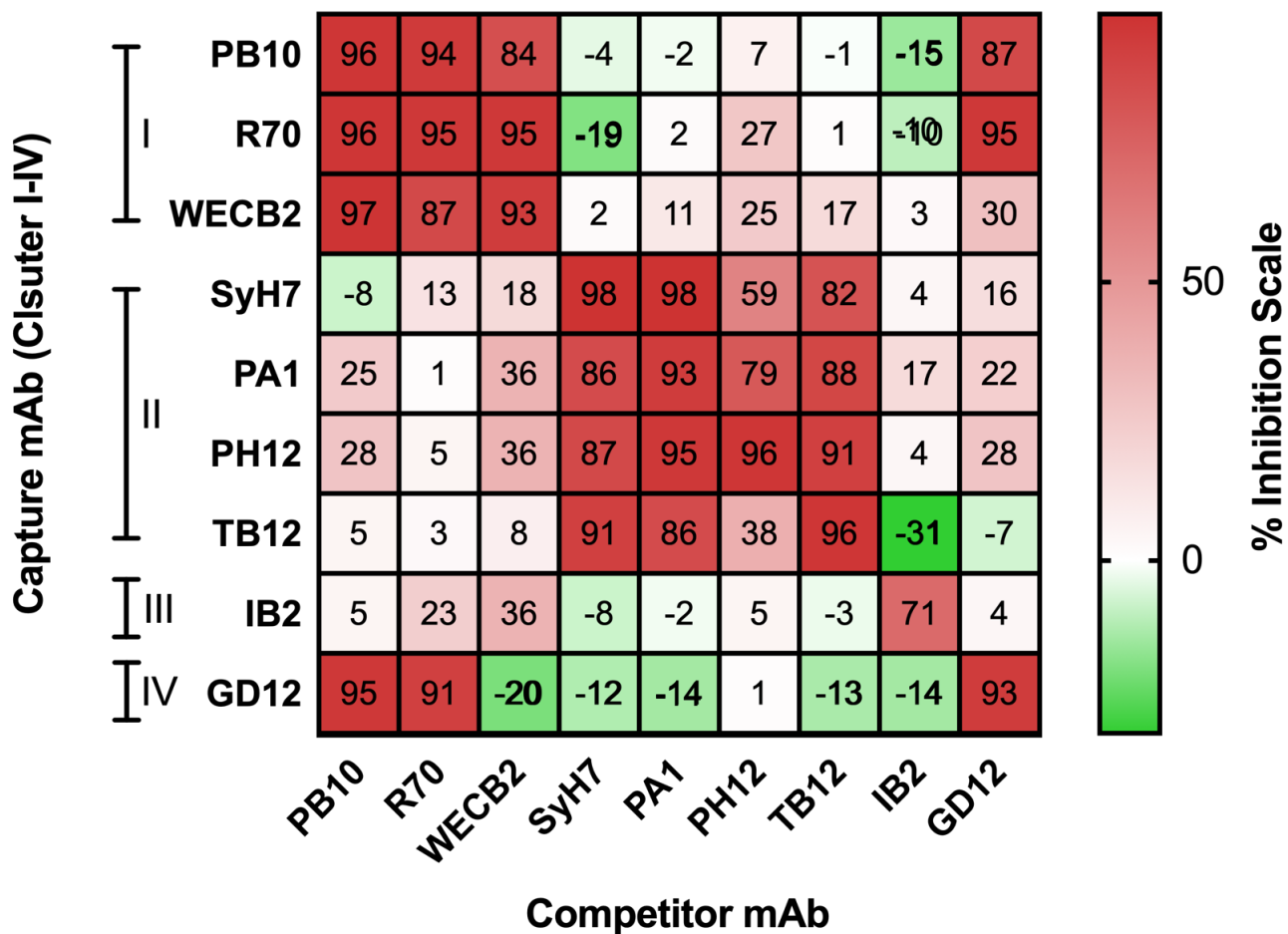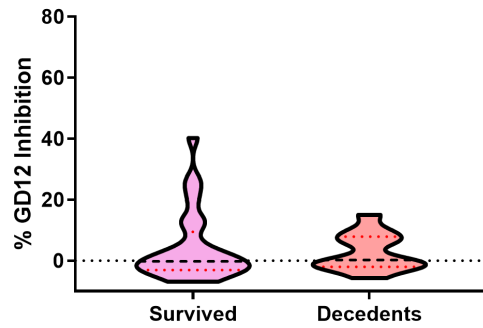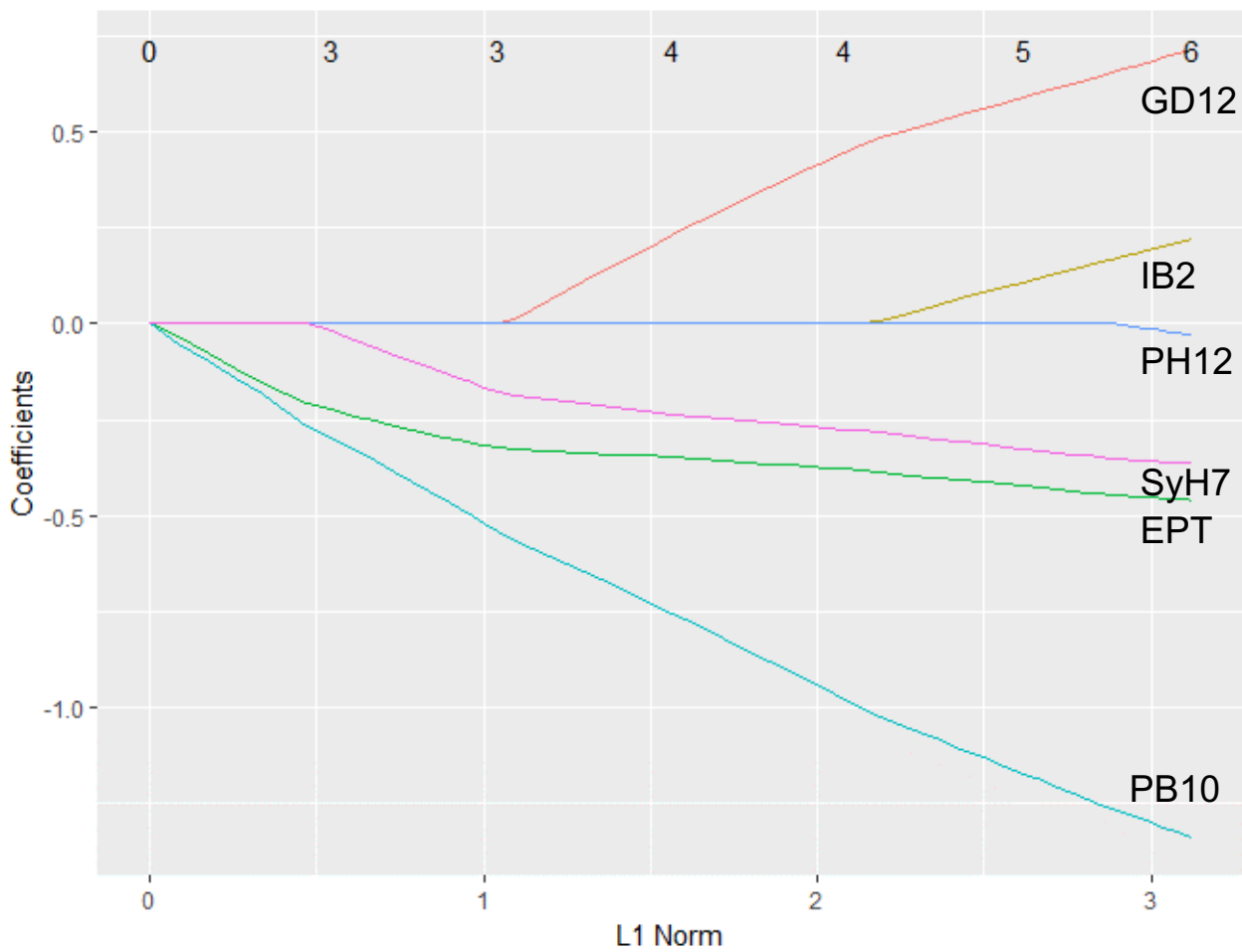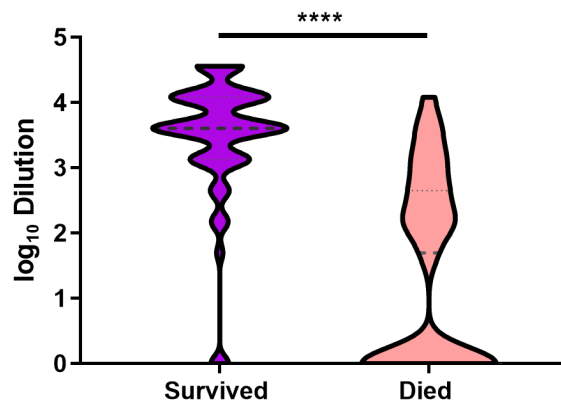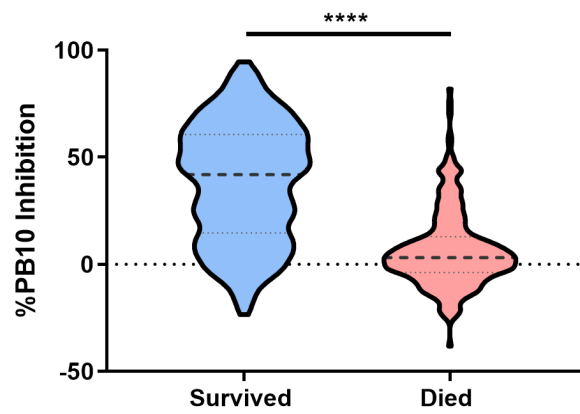
Figure 2
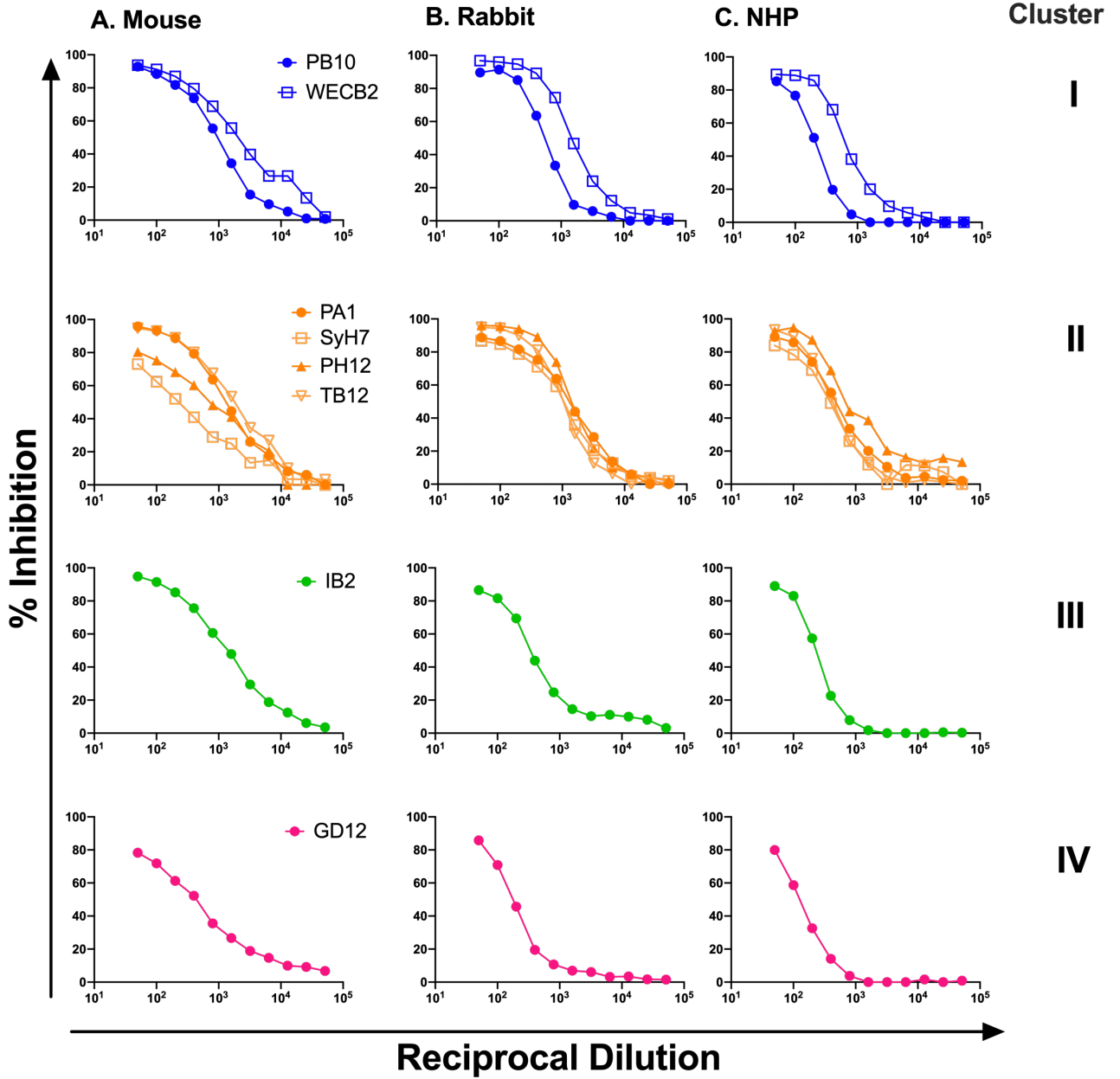
Figure 3
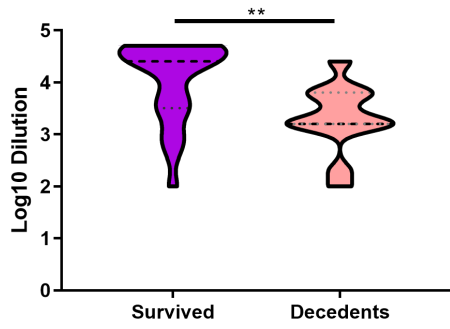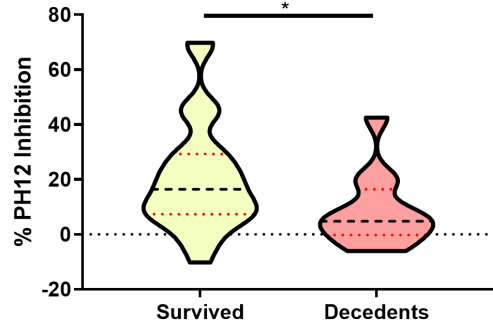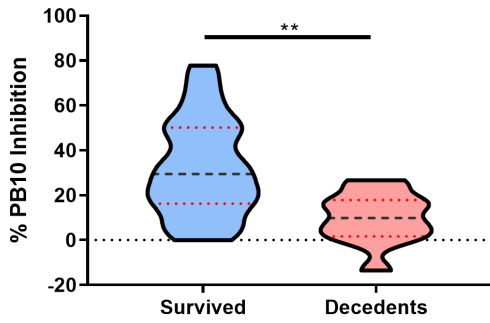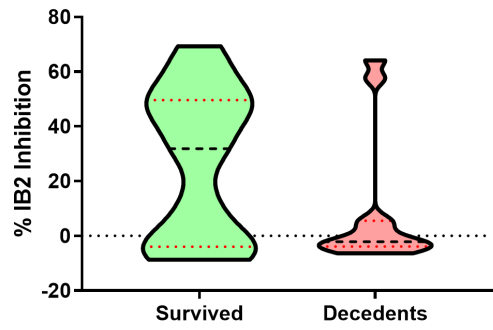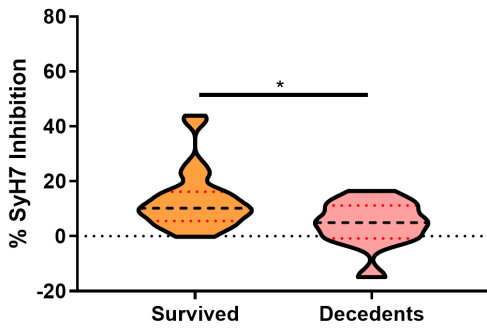
Figure 4

Figure 5

A. End-Point Titer

B. PB10

C. SyH7

Figure 6

MAb	AUC	95% CI
SyH7	0.796	0.7619-0.8301
PB10	0.8155	0.783-0.848
EPT	0.8649	0.8369-0.893